

行政院國家科學委員會專題研究計畫 成果報告

5~6 GHz 頻段室內寬頻／超寬頻無線通道量測與模擬(3/3)

計畫類別：個別型計畫

計畫編號：NSC93-2213-E-009-020-

執行期間：93年08月01日至94年07月31日

執行單位：國立交通大學電信工程學系(所)

計畫主持人：唐震寰

報告類型：完整報告

報告附件：出席國際會議研究心得報告及發表論文

處理方式：本計畫可公開查詢

中華民國94年11月4日

# 5~6 GHz 頻段室內寬頻／超寬頻無線通道量測與模擬(3/3)

## 5~6 GHz Wideband / Ultra-wideband Radio Measurement and Channel Modeling for Indoor Environments (3/3)

計畫編號：NSC93-2213-E009-020

執行期限：93 年 8 月 1 日至 94 年 7 月 31 日

主持人：唐震寰 國立交通大學電信工程學系

### 中文摘要

超寬頻無線技術由於其高傳輸容量、不易受多重路徑影響、具備精密的定位及測距能力、以及不易被截取等優點，近年來在科學、工業、通信及軍事等領域上都獲得相當大的重視，歐美各國也都相繼投入其應用研發。為瞭解超寬頻信號在室內的通道特性，本計畫乃規劃以掃頻量測方法，量測及探討其室內傳播特性。本計畫將於三年內進行兩階段之研究工作：(1) 第一階段(第一及第二年)：對超寬頻信號傳播路徑損耗、衰落、及功率延遲分佈等特性進行量測與模型建構及驗證；(2) 第二階段(第三年)：以第一階段的研究結果應用於在探討超寬頻信號在室內無線傳播特性。

在計畫執行的第一年中，我們完成了超寬頻室通道量測系統的架設，以此系統對 5~6 GHz 寬頻信號在室內的傳播特性進行量測。同時，也以所發展的三維適應環境性傳播模型及射線追蹤技術來模擬此一頻段的無線信號在室內環境的傳播現象。為能獲得較合理的模擬結果，研究中同時也對一般室內建材在超寬頻頻段的介電係數進行量測，並將所測得的介電係數用於模擬中。經比較量測與模擬所得的數據，証實了此傳播模型之有效性與正確性。

計畫執行的第二年，我們以預估延遲拍線模型為基礎，對室內超寬頻信號功率延遲分佈的相關參數如時間延遲係數和功率損耗率等進行分析。同時也推導出時間延遲係數和功率損耗率與信號頻寬的關係式，可用以預測室內環境中不同頻寬信號的功率延遲分佈特性。研究中也以所架設之超寬頻脈衝響應量測系統，在不同條件的室內環境下進行了大量的量測。經與量測結果比較後，也驗證了所推導模型的正確性，並且得到兩項結果：(1) 同一傳播環靜中，信號的頻寬並不會對平均功率延遲分佈的時間延遲係數造成影響；(2) 同一傳播環靜中，平均功率延遲分佈的功率損耗率會隨著信號頻寬的增加而減少。

本年度為計畫的第三年，我們藉由 Stochastic tapped-delay-line (STD L) 模型，完成室內超寬頻無線通道參數隨頻率變動之公式推導。該模型利用衰減常數 (delay constant)、電功率比值 (power ratio) 及 Nakagami 常數描述通道特徵。如給定窄頻通道特徵參數值，可利用上述公式計算超寬頻通道特徵參數值。該研究成果經與在實驗室、辦公室及教室內大量實測結果 (3GHz~5GHz) 驗證，顯示良好之預估準確性。實測結果同時顯示通道特徵參數與頻寬之關係：(1) 電功率比值隨著頻寬之增加而變大；(2) 衰減常數與頻寬似乎無關；及 (3) Nakagami 常數也隨著頻寬之增加而變大。

整體而言，感謝國科會之研究補助使本多年期研究計畫得以順利執行並完成。目前已投稿一篇 IEEE Trans. on Vehicular Technology (under revised)、一篇

IEEE Trans. on Wireless Communications，以及數篇國際會議論文。

關鍵詞：超寬頻、無線電傳播、通道響應、STD L 模型、頻寬效應

### Abstract

Ultra Wideband (UWB) radio techniques have recently attracted great interest in scientific, industrial, commercial, and military sectors. The potential strength of the UWB radio technique such as high channel capacity at short range, lack of significant multipath fading, accurate position location and ranging, and extremely difficult to intercept, lies in its use of extreme wide transmission bandwidths.

In this project, a spectrum analyzing and a swept frequency measurement methods are adopted to measure and to analyze the UWB radio propagation loss, multi-path fading, signal delay and spread. It is a three years project and is separated into two stages. (1) The first stage (1st and 2nd years): measurement and modeling of the UWB radio propagation loss, multi-path fading, and power delay profile; (2) The second stage (3rd year): investigation of UWB indoor propagation characteristics.

In the last annual report, an ultra wideband channel sounding system and a swept frequency measurement method are adopted to measure and to analyze UWB radio wave propagation characteristics in indoor environment. A site-specific model using ray-tracing technique is developed to predict the radio propagation in indoor environments. Simulation results are validated by the experimental results.

In the second year, the stochastic tapped-delay-line (STD L) model is introduced to model the UWB indoor channels with the parameters, delay constant and power ratio, of the averaged power-delay profile (PDP). Here, the formulas of these two parameters versus signal bandwidth are proposed. The formulas have been validated by comparing the computed results with a large number of measurement data carried out at many sites such as classrooms, laboratories and offices. The measured frequencies are ranged from 3 GHz to 5 GHz. It is found that (1) The delay constant of the averaged PDP is independent of radio bandwidth; (2) The power ratio of the averaged PDP is decreased when the

radio bandwidth is increased.

In the third year, modeling dependency of Ultra-Wideband (UWB) indoor radio channel parameters on bandwidth is explored. Here, formulas describing these dependencies are derived under the stochastic tapped-delay-line (STDL) model, which characterizes radio channels using parameters such as decay constant, power ratio and Nakagami parameter. Through these formulas, the proper UWB channel parameters for a ultra-wide bandwidth signal can be determined from those of a narrow bandwidth signal. These formulas have been validated by comparing the computed results with a large number of measurement data carried out at laboratories, offices and classrooms. The measured frequencies are ranged from 3 GHz to 5 GHz. It is found that (1) The power ratio is decreased when the signal bandwidth is increased; (2) The decay constant is independent of radio bandwidth; and (3) The Nakagami parameter is increased as the signal bandwidth is increased.

As a whole, with these research achievement, we had submitted one paper to IEEE Trans. on Vehicular Technology (in revised), another paper to IEEE Trans. on Wireless Communications, and some presentations at international conferences.

Keywords: UWB, radio propagation, channel impulse response, STDL model, bandwidth effect.

## I. Introduction

Ultra-Wideband (UWB) radio techniques have recently attracted great interest in scientific, industrial, commercial, and military sectors. The potential strength of the UWB radio technique such as high channel capacity at short range, lack of significant multipath fading, accurate position location and ranging, and robustness to interception, lies in its use of extreme wide transmission bandwidths [1]. According to the Federal Communication Commission (FCC) regulations of UWB radio technology and systems [2], the minimum bandwidth limit of an UWB radio signal is 500 MHz, and the frequency band from 3.1 GHz to 10.6 GHz is available for unlicensed use for indoor communication applications. Due to its extremely wide bandwidth, each UWB system achieves very high resolution in the delay domain. Therefore, the UWB channel response may contains several tens to hundreds multipath components (MPCs), which are very different from those of conventional narrowband/broadband indoor wireless communication systems. Therefore, precise multipath models are of primary importance to the UWB channel models.

It is noted that for band-limited radio systems, the signal resolution, proportional to the

inverse of the bandwidth, affects the number of resolvable MPCs and their powers, and of course changes values of the channel response parameters as well. It is important to find the dependency of channel parameters on signal bandwidth for UWB radio systems since their signal bandwidth may vary in a wide range to provide manifold applications with varying data rate and quality of services requirements. In theory, channel responses of narrowband signals may be derived from that of wideband signals by a simple bandpass filtering operation, but it is difficult to estimate the channel responses of any wideband signal from those of a narrowband signal.

In this paper, modeling dependency of UWB indoor radio channel parameters on bandwidth is explored. Here, the formulas describing these dependencies are derived under the stochastic tapped-delay-line (STDL) model [3], which characterizes radio channels using parameters such as decay constant, power ratio and Nakagami parameter. Through these formulas, the proper UWB channel parameters for a wide bandwidth signal can be determined from those of a narrow bandwidth signal.

This paper is organized as follows. In Section II, the STDL model that we adopted to characterize the indoor UWB radio propagation channel is presented. The dependency of channel parameters on bandwidth are analyzed and derived in Section III. In Section IV, the measurement system and environments are described. Results of our finding are validated by measurement data in Section V. Conclusions are given in Section VI.

## II. The STDL Channel Model

Because of multipath propagation due to reflections, refractions, and/or scattering by obstacles or scatters in propagation environments, radio propagation channels are usually modeled as a linear filter with a complex-valued lowpass equivalent impulse response that is expressed as

$$h(\tau) = \sum_k a_k \delta(\tau - \tau_k) \quad (1)$$

where  $a_k$  and  $\tau_k$  are the random complex-valued path gain and propagation delay of the MPCs, respectively; and  $\delta$  is the Dirac delta function.

To characterize the statistical properties of UWB indoor channels, the STDL model was proposed by Win et al [3]. It characterizes the shape of the power delay profile (PDP) of the UWB indoor channel in terms of power gains and delays of taps, i.e, by the pairs  $\{P_i, \tau_i\}$  with  $\tau_i = (i-1) \times \Delta$ , where  $\Delta$  is the tap spacing and is equal to signal resolution of the considered

system. Meanwhile,  $P_i$  is equal to the square of the vectorial sum of the arriving MPCs over a tap spacing beginning at the delay  $(i-1)\times\Delta$ , i.e.,  $P_i=|\sum a_k|^2$ , for  $(i-1)\times\Delta\leq\tau_k<i\times\Delta$ .

In the model, the small-scale averaged PDP,  $\bar{P}(\tau)$ , is modeled by a single exponential (linearly on a decibel scale) PDP with a stronger first tap as shown in Fig. 1 and is expressed as

$$\bar{P}(\tau)=\delta(\tau)+\sum_{i=2}^L r \exp\left(-\frac{(i-2)\times\Delta}{\varepsilon}\right)\delta(\tau-(i-1)\times\Delta) \quad (2)$$

where  $L$  is the total number of taps in the observation window,  $\varepsilon$  is the exponentially power decay constant and  $r$  is the power ratio that is defined as the ratio of the averaged power of the second tap to the first tap, i.e.,  $r=\bar{P}_2/\bar{P}_1$ . It is noted that,  $\bar{P}_i$  is the  $i^{\text{th}}$  tap's power normalized to the power of the first tap, i.e.,  $\bar{P}_1=1$ .

The small-scale statistics of each tap's power gain follows a Gamma distribution (Nakagami envelope distributed), and each Nakagami parameter,  $m$ , is described by a truncated-Gaussian random variable with its mean and standard deviation decreasing with delay.

To sum up, STDL model is completely characterized by three parameters, the *decay constant*  $\varepsilon$ , the *power ratio*  $r$ , and the *Nakagami parameter*  $m$ . It is noted that these parameters are not only dependent on the propagation environment and maybe dependent on the signal bandwidth of the considered system.

### III. Formulation of Channel Parameters

To explore bandwidth dependency of these channel parameters, the formulas to determine UWB indoor channels parameters of a wide bandwidth signal with those of a narrow bandwidth signal are derived. It is noted that the bandwidth of the wideband signal is confined and is  $2^n$  times of that of the narrowband signal. For the convenience of description in the following of this paper, the parameters with index  $f$  or  $F$  correspond to those of bandwidth  $f$  or  $F$ , respectively, where  $F=2\times f$ .

#### A. Bandwidth on Decay Constant and Power Ratio

Since tap spacing is inversely proportional to the signal bandwidth,  $\Delta_f$ , the tap spacing of a system with signal bandwidth  $f$ , is equal to  $2\times\Delta_F$ , two times of that of a system with signal bandwidth  $F$ . Therefore,  $\bar{P}_i(f)$ , the power gain of the  $i^{\text{th}}$  tap of a signal with bandwidth  $f$ , is resulted from the combination of MPCs arriving within taps  $2i-1$  and  $2i$  of signals with bandwidth  $F$ .

For an uncorrelated scattered radio propagation channel [4], the amplitudes of the taps are independently to one other. Therefore, the

small-scale averaged tap power gain can be calculated as the sum of the power of MPCs arriving within a tap spacing of the corresponding tap. From the results shown in [3], it reveals that the uncorrelated scattering assumption can be applied to the indoor UWB radio propagation channels. Therefore,  $\bar{P}_i(f)$ , the small-scale averaged power gain of the  $i^{\text{th}}$  tap of a signal with bandwidth  $f$ , can be calculated as the sum of  $\bar{P}_{2i-1}(F)$  and  $\bar{P}_{2i}(F)$ . From (2),  $\bar{P}_i(f)$  is expressed as

$$\begin{cases} \bar{P}_1(f)=\bar{P}_1(F)+\bar{P}_2(F)=1+r_F \\ \bar{P}_i(f)=\bar{P}_{2i-1}(F)+\bar{P}_{2i}(F), & i\geq 2 \\ =r_F\times\left\{\exp\left[-\frac{(2i-3)\times\Delta_F}{\varepsilon_F}\right]+\exp\left[-\frac{(2i-2)\times\Delta_F}{\varepsilon_F}\right]\right\} \\ =r_F\times\left[\exp\left(-\frac{\Delta_F}{\varepsilon_F}\right)+\exp\left(-\frac{2\times\Delta_F}{\varepsilon_F}\right)\right]\times\exp\left(-\frac{(i-2)\times\Delta_f}{\varepsilon_F}\right) \end{cases} \quad (3)$$

From (3), it is found that the  $\bar{P}_i(f)$  is exponentially decayed with time decay constant  $\varepsilon_F$ . It represents that the decay constant is not dependent on the bandwidth, i.e.,  $\varepsilon_f=\varepsilon_F$ . By normalizing all the taps' power,  $\bar{P}_i(f)$ , to the power of the first tap,  $\bar{P}_1(f)$ , it is found that power ratio  $r_f$  can be determined by  $r_F$ ,  $\varepsilon_F$  and  $\Delta_F$  by (4)

$$\begin{aligned} r_f &= \frac{r_F}{1+r_F}\times\left[\exp\left(-\frac{\Delta_F}{\varepsilon_F}\right)+\exp\left(-\frac{2\times\Delta_F}{\varepsilon_F}\right)\right] \\ &\approx \frac{2\times r_F}{1+r_F}, \quad \text{if } \Delta_F \ll \varepsilon_F \end{aligned} \quad (4)$$

From (4), it is found that  $r_f$  is greater than  $r_F$  under the condition that if  $\varepsilon_F \gg \Delta_F$ . The indoor UWB channels, for the most part, satisfy this condition with a typical decay constant larger than 10ns and tap spacing smaller than 2ns. Furthermore, from (4) and the condition  $\varepsilon_f=\varepsilon_F$ , it is also found that  $r_F$  can be determined by  $r_f$ ,  $\varepsilon_f$  and  $\Delta_f$  by (5)

$$\begin{aligned} r_F &= \frac{r_f}{\left[\exp\left(-\frac{1/2\times\Delta_f}{\varepsilon_f}\right)+\exp\left(-\frac{\Delta_f}{\varepsilon_f}\right)\right]-r_f} \\ &\approx \frac{r_f}{2-r_f}, \quad \text{if } \Delta_f \ll \varepsilon_f \end{aligned} \quad (5)$$

#### B. Bandwidth on Nakagami Parameter

To explore the Nakagami parameter dependency on bandwidth, a Rician distribution is used to replace the Nakagami distribution as that in the STDL model [3]. It is because the Rician distribution yields more physical meaning by characterizing the ratio of the specular/LOS path power (coherent power) to the scattered MPCs (incoherent power) with a Rician factor. It is helpful to derive the formula describing the bandwidth dependency of small-scale fading statistics. Meanwhile, it is noted that these two

distributions can be transformed into each other via the following relations between the Rician factor  $K$  and the Nakagami parameter  $m$  [5]

$$K = \sqrt{m^2 - m} / (m - \sqrt{m^2 - m}) \quad (6a)$$

$$m = (K + 1)^2 / (2K + 1) \quad (6b)$$

Rician factor is defined as the ratio of the power of the specular/LOS path and the other scattered MPCs. Here, let  $A^2$  and  $2\sigma^2$  be the average power of the specular/LOS path and the other scattered multipaths of the first tap for bandwidth  $F$ , respectively. Since  $\bar{P}_1(f) = \bar{P}_1(F) + \bar{P}_2(F)$ , the average power of scattered multipaths of the first tap for radio bandwidth  $f$  is equal to the sum of  $2\sigma^2$  and  $\bar{P}_2(F)$ . Then the Rician factor  $K_f$  can be calculated by (7)

$$K_f = \frac{A^2}{2\sigma^2 + \bar{P}_2(F)} = \frac{\frac{K_F}{K_F+1} \times \bar{P}_1(F)}{\frac{1}{K_F+1} \times \bar{P}_1(F) + r_F \times \bar{P}_1(F)} \quad (7)$$

$$= \frac{K_F}{1 + (K_F + 1) \times r_F}$$

From (7), it is easily to find that  $K_f$  is smaller than  $K_F$ , which is due to the fact that the numbers of scattered MPCs fall within the first tap is decreased when the signal bandwidth is increased, i.e., yielding a decrease of the scattered power. Substituting (5) into (7),  $K_f$  is expressed in terms of  $K_F$ ,  $r_f$ ,  $\varepsilon_f$  and  $\Delta_f$  as the following equation

$$K_f = \frac{K_F \times \left( 1 + \frac{r_f}{\exp(-0.5 \times \Delta_f / \varepsilon_f) + \exp(-\Delta_f / \varepsilon_f)} - r_f \right)}{1 - K_F \times \frac{r_f}{\exp(-0.5 \times \Delta_f / \varepsilon_f) + \exp(-\Delta_f / \varepsilon_f)} - r_f} \quad (8)$$

Therefore,  $m_f$ , the Nakagami parameter for bandwidth  $F$  can be estimated through the following procedures:

- 1) To translate  $m_f$  into  $K_f$  by (6a),
- 2) To compute  $K_F$  by (8),
- 3) To translate  $K_F$  into  $m_F$  by (6b).

#### IV. Measurement Setup and Environment

In our study, the frequency domain measurement technology to perform UWB indoor channel sounding is adopted. A Vector Network Analyzer (VNA) was used to record the variation of 801 complex tones across the 3-5 GHz frequency ranges. The time-domain channel responses are obtained by taking the inverse Fourier transform of the frequency-domain channel response.

UWB propagation experiments were performed in three different floors of Engineering Building Number Four at the National Chiao-Tung University in Hsin-Chu, Taiwan. Figs. 2(a)-(d) show the floor layouts of the

measurement sites including a laboratory, a classroom, a computer room, and corridors/classrooms, respectively. Room #901 is a laboratory with some equipments and iron tables. The classroom has many wooden chairs and the computer room has ten iron tables and fifty computers. At these sites, all measured points are under the Line-of-Sight (LOS) condition. At the last site, the transmitter (Tx) is located at the corridor and 15 measured points are carefully planned to include LOS and non-LOS (NLOS) propagations. At each measured point, 64 channel frequency responses were sampled at 64 sub-points, arranged in  $8 \times 8$  square grid, as shown in Fig. 2(d). The spacing between two neighboring sub-points is 3.75 cm. In each measurement, both the transmitting and receiving antennas are fixed with the same height of 1.6 m.

Here, we classify the total 24 measurement points into four propagation cases according to the LOS/NLOS condition and distance between the transmitter and the receiver. Case 1 is for LOS condition and short T-R distance (0-5m) case, and it includes the measurement points no.1-no.6. Case 2 is also for LOS condition but with longer T-R distance (5-10m), and it includes the measurement points no.7-no.12. Case 3 is for NLOS condition and short distance (0-5m) case, and it includes the measurement points no.13-no.18. Case 4 is also for NLOS condition but with longer T-R distance (5-20m), and it includes the measurement points no.19-no.24.

#### V. Validation and Discussion

All the measured frequency-domain channel responses is processed to time-domain by taking the inverse Fourier transform and obtained  $24 \times 64$  different PDPs. Since the absolute propagation delays of the received signals vary from one point to another, an appropriate delay reference is needed to characterize the relative delays of each MPC. Here we translate the delay axis of the PDP for each measurement point by its respective absolute delay of the directed path between transmitter and receiver. In the following, we refer to the PDP measured at one of the  $24 \times 64$  subpoints as local PDP, while we denote the PDP averaged over the 64 subpoints of one measurement point as the small-scale averaged PDP (SSA-PDP). We performed best-fit procedures to extract the channel parameters,  $\varepsilon$ 's and  $r$ 's, from the SSA-PDP of each measurement point. The other channel parameter  $m$ 's are obtained by fitting the CDF of the deviations of the 64 1<sup>st</sup> tap's path gain to that of a Gamma distribution (Nakagami envelop distributed) for each measurement point.

### A. Decay Constant

Fig. 3 shows the decay constant of each measured point for signal bandwidths of 500 MHz, 1 GHz and 2 GHz. It is found that the decay constant is slightly dependent on the signal bandwidth with similar results of these three bandwidths at each point. This result is consistent with our analytical result as shown in (3). The mean decay constants of cases 1-4 are 7ns, 12ns, 8ns and 22ns, respectively. It reveals that the mean decay constant tends to increase with the propagation distance. This is because that as the propagation distance is increased, the ratio of the propagation distance of each subsequent MPCs to that of the direct path is decreased, and it leads to larger power gains for delay taps.

### B. Power Ratio

Fig. 4 shows the power ratio of each measurement point for signal bandwidths of 500 MHz, 1 GHz and 2 GHz. It is found that the power ratio is decreased when the signal bandwidth is increased, which validates our analytical result as shown in (4). Fig. 5 shows the measured and computed power ratio of each measurement point for 1 GHz bandwidth. Here, the computed results are based on the measured results of a 500MHz-bandwidth signal and using (5). The comparison shows that our proposed method yields good prediction accuracy of power ratio with  $\bar{E}_r(500 \text{ MHz}, 1 \text{ GHz}) = 0.0704$ . Here,  $\bar{E}_r(f_1, f_2)$ , represents the mean of the relative prediction error (the ratio of the difference between the predicted and the measured data to the measured data) of power ratio and is given by

$$\bar{E}_r(f_1, f_2) = \left| \frac{1}{N} \sum_{j=1}^N (r_p(j, f_1, f_2) - r_m(j, f_2)) / r_m(j, f_2) \right| \quad (9)$$

where  $r_p(j, f_1, f_2)$  is the computed power ratio of the  $j^{\text{th}}$  measurement point for bandwidth  $f_2$  and it is predicted from the measured results of a signal with bandwidth  $f_1$ .  $r_m(j, f_2)$  are the measured power ratio of  $j^{\text{th}}$  measurement point for bandwidth  $f_2$ . For conciseness, the computed results of power ratio for bandwidths (1 GHz, 2 GHz) and (500 MHz, 2 GHz) with  $\bar{E}_r(1 \text{ GHz}, 2 \text{ GHz}) = 0.1129$  and  $\bar{E}_r(500 \text{ MHz}, 2 \text{ GHz}) = 0.1635$ , respectively, are not illustrated.

### C. Nakagami Parameter

From our measurement evidence, it is found that the Nakagami parameters, except the first tap, are all closed to 1 (Rayleigh distribution). Therefore, we only focus on the Nakagami parameter of the first tap in this paper. Fig. 6

shows the Nakagami parameter for all the 24 measurement points for signal bandwidths of 500 MHz, 1 GHz and 2 GHz. It is found that the Nakagami parameter is increased when the signal bandwidth is increased, which validates our analytical result. Fig. 7 shows the measured and computed Nakagami parameter of each measurement point for 1 GHz bandwidth. Here, the computed results are based on the measured results of a 500MHz-bandwidth signal. The comparison shows that our proposed method yields good prediction accuracy of Nakagami parameter.

To quantify the prediction accuracy of the Nakagami parameter, the mean of the relative prediction error of Nakagami parameter,  $\bar{E}_m(f_1, f_2)$ , is defined and given by

$$\bar{E}_m(f_1, f_2) = \left| \frac{1}{N} \sum_{j=1}^N (m_p(j, f_1, f_2) - m_m(j, f_2)) / m_m(j, f_2) \right| \quad (10)$$

where  $m_p(j, f_1, f_2)$  is the computed Nakagami parameter of the  $j^{\text{th}}$  measurement point for bandwidth  $f_2$  and it is predicted from the measured results of a signal with bandwidth  $f_1$ .  $m_m(j, f_2)$  are the measured Nakagami parameter of  $j^{\text{th}}$  measurement point for bandwidth  $f_2$ . After some computations,  $\bar{E}_m(f_1, f_2)$  are equal to 0.3690, 0.1507 and 0.2412 for  $(f_1, f_2)$  equal to (500 MHz, 1 GHz), (1 GHz, 2 GHz) and (500 MHz, 2 GHz), respectively.

## VI. Conclusions

In this paper, the formulas describing bandwidth dependency of UWB channel parameters, such as power ratio, decay constant and Nakagami parameter, are derived under the STDL model. These formulas have been validated by comparing the computed results with a large number of measurement data carried out at laboratories, offices and classrooms with frequencies ranged from 3 GHz to 5 GHz and signal bandwidths of 500 MHz, 1 GHz and 2 GHz. Through these formulas, the values of UWB channel parameters for wide bandwidth signals can be determined from those of narrow bandwidth signals.

In the future, we plan to investigate the bandwidth dependency of channel parameters of S-V model. It is a well-recognized model to characterize the multipath-clustering phenomenon that may be observed in UWB indoor radio channels especially when the signal bandwidth is extended to several GHz.

## References

- [1] Porcino and W. Hirt, "Ultra-Wideband Radio Technology: Potential and Challenges Ahead," IEEE Communications Magazine, vol.41, issue 7, July 2003, pp.66-74.
- [2] FCC "Revision of Part 15 of the Commission's Rules Regarding Ultra-Wideband Transmission Systems," First Report and Order, ET Docket 98-153, FCC 02-48, Apr. 2002.
- [3] Dajana Cassioli, Moe Z. Win, Andreas F. Molisch, "The Ultra-Wide Bandwidth Indoor Channel: From Statistical Model to Simulations," IEEE Journal on Selected Areas in Communications, vol. 20, no.6, Aug. 2002, pp. 1247-1257.
- [4] J. D. Parsons, "The Mobile Radio Propagation Channel," Pentech Press Publishers, London, 1992.
- [5] M. Nakagami, "The m distribution; a general formula of intensity distribution of rapid fading," Statistical Methods in Radio Wave Propagation, W.G. Hoffman, ed., pp. 3-36, 1960

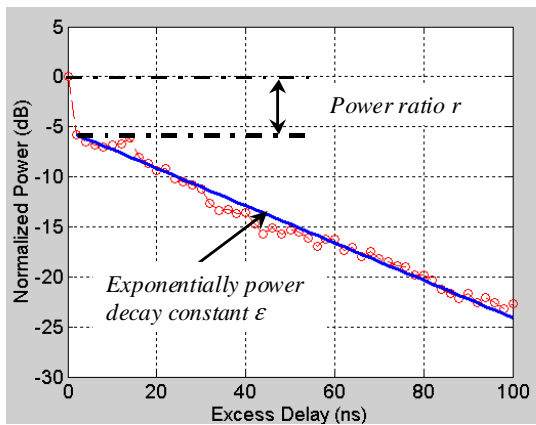


Fig. 1 The averaged power delay profile of a 500MHz-bandwidth UWB signal, which is measured in an indoor environment under NLOS condition.

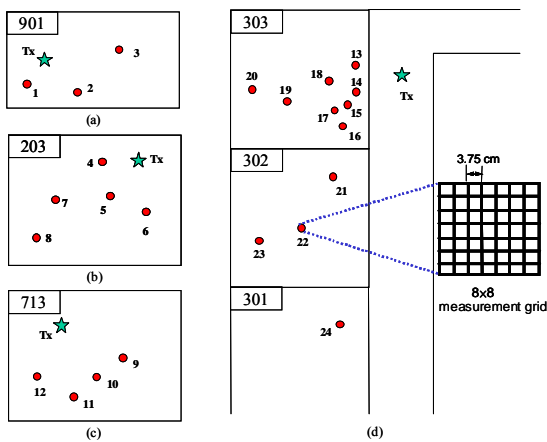


Fig. 2 Layouts of four measurement sites. (a) laboratory 901; (b) classroom 203, (c) computer room 713; (d) classrooms 301-303.

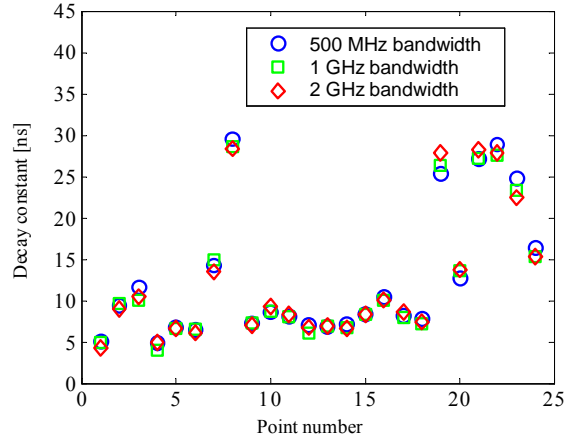


Fig.3 Decay constant versus measurement point number for signal bandwidths of 500 MHz, 1 GHz, and 2 GHz.

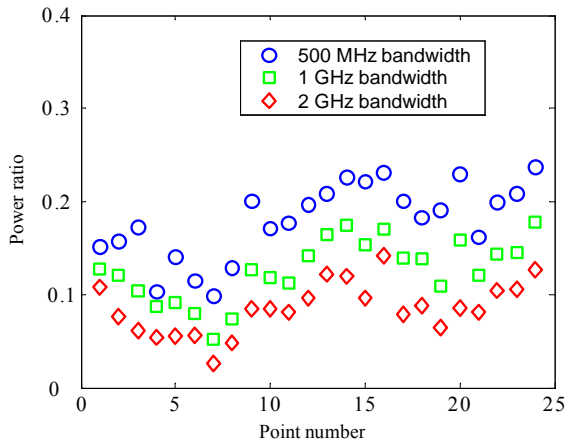


Fig.4 Power ratio versus measurement point number for signal bandwidths of 500 MHz, 1 GHz, and 2 GHz.

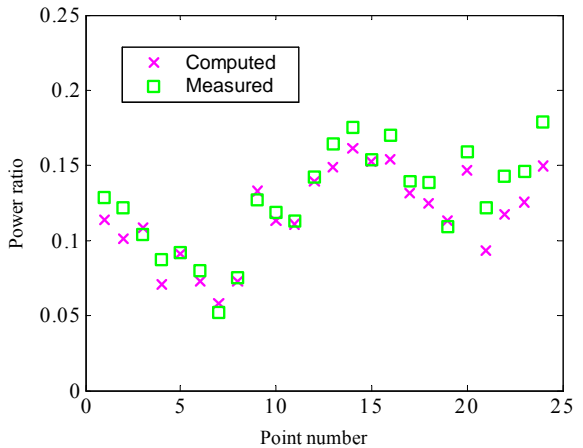


Fig.5 Comparisons between the measured and computed results of the power ratio for all of the 24 measurement points at 1 GHz bandwidth

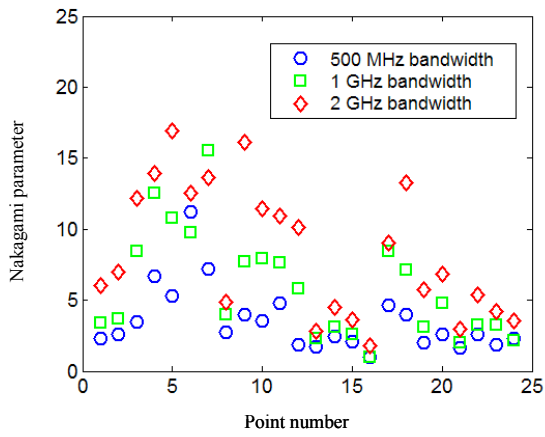


Fig. 6 Nakagami parameter versus measurement point number for signal bandwidths of 500 MHz, 1 GHz, and 2 GHz.

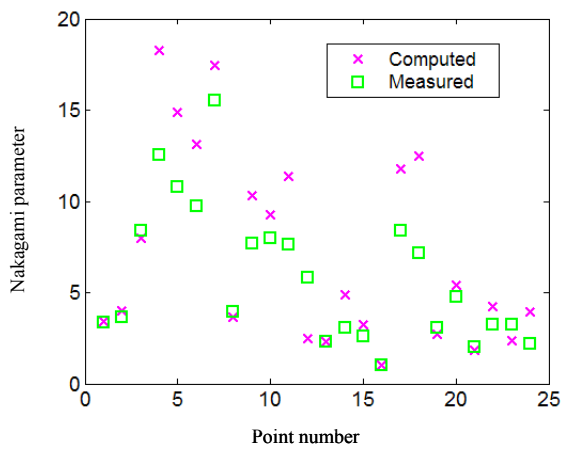


Fig.7 Comparisons between the measured and computed results of the Nakagami parameter for all of the 24 measurement points at 1 GHz bandwidth.